Supporting Information

Cellulose Nanocrystals as Anti-Oil Nanomaterials for Separating Crude Oil from Aqueous Emulsions and Mixtures

Ming-Bang Wu[†], Chao Zhang[†], Jun-Ke Pi, Chang Liu, Jing Yang[*] and Zhi-Kang Xu[*]

M.-B. Wu, C. Zhang, J.-K. Pi, C. Liu, Dr. J. Yang, Prof. Z.-K. Xu
MOE Key Laboratory of Macromolecular Synthesis and Functionalization, and Key Laboratory of Adsorption and Separation Materials & Technologies of Zhejiang Province, Department of Polymer Science and Engineering, Zhejiang University, Hangzhou 310027, China
E-mail: jing_yang@zju.edu.cn,xuzk@zju.edu.cn
[†] The two authors contributed equally to this work

Table S1 Surface composition of the microcrystalline cellulose and the cellulose nanocrystal from XPS spectra (in atomic percent).

Sample	C (%)	O (%)	S (%)
Microcrystalline cellulose	60.1	39.9	0
Cellulose nanocrystal	57.39	41.76	0.85

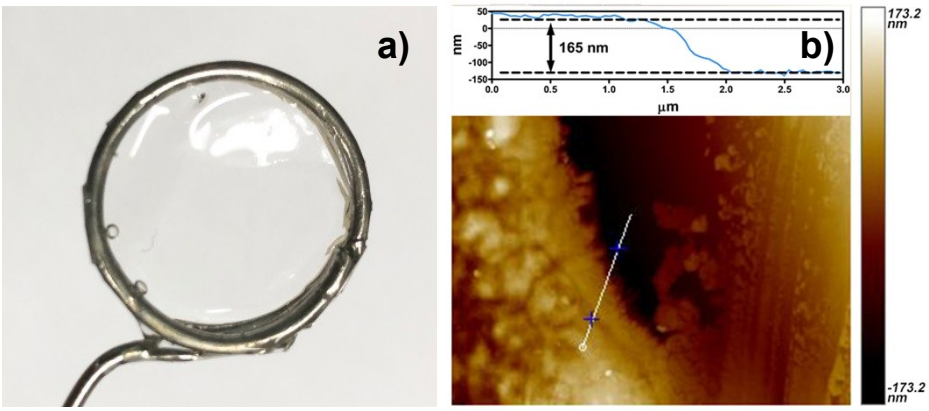

Figure S1 a) Digital photo of the free-standing CNCs-based nanopapers after removing the poly(ether sulfone) substrate. b) AFM image and height profile of the CNCs-based nanopapers.

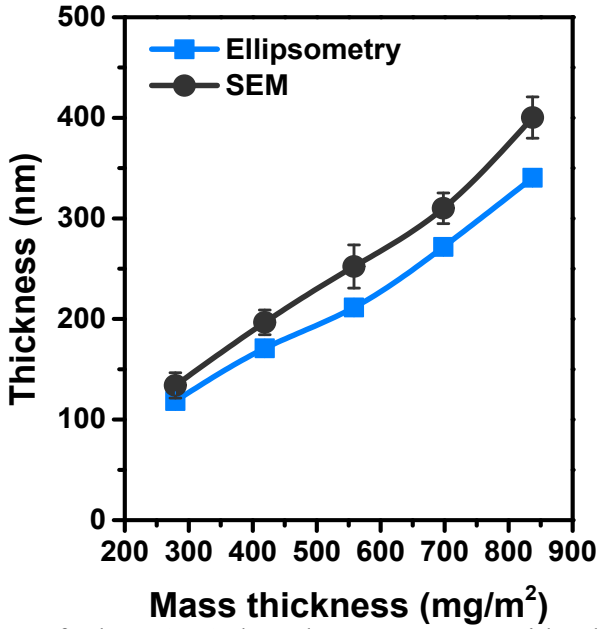

Figure S2 Thickness of the CNCs-based nanopapers with different CNCs mass thicknesses.

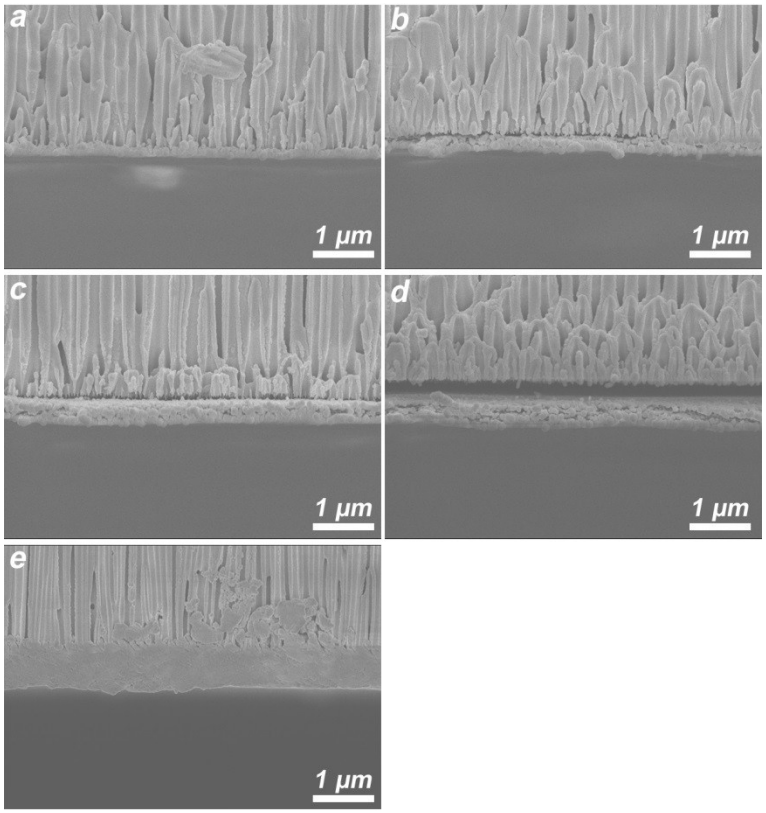

Figure S3 Cross-sectional morphologies of CNCs/AAO composite membranes with different CNCs mass thicknesses. a) 0 mg m^{-2}, b) 280 mg m^{-2}, c) 420 mg m^{-2}, d) 560 mg m^{-2}, e) 700 mg m^{-2} and f) 840 mg m^{-2}, respectively.

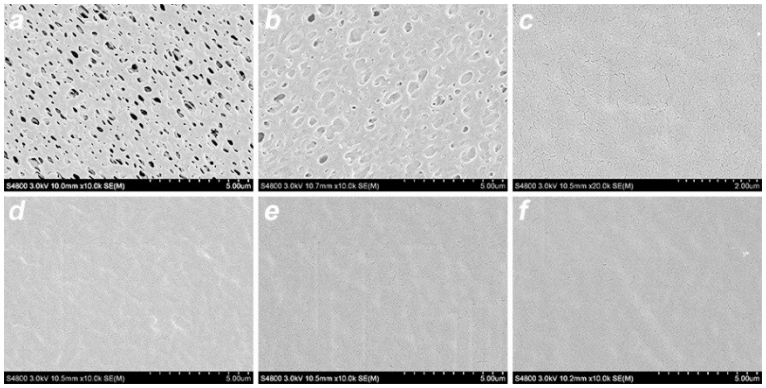

Figure S4 Surface morphologies of CNCs/poly(ether sulfone) composite membranes with different CNCs mass thicknesses. a) 0 mg m^{-2}, b) 280 mg m^{-2}, c) 420 mg m^{-2}, d) 560 mg m^{-2}, e) 700 mg m^{-2} and f) 840 mg m^{-2}, respectively.

Figure S5 A series of photos taken when a water droplet was approaching the CNCs-based nanopapers surface. The mass thickness of CNCs is 428 mg m^{-2}.

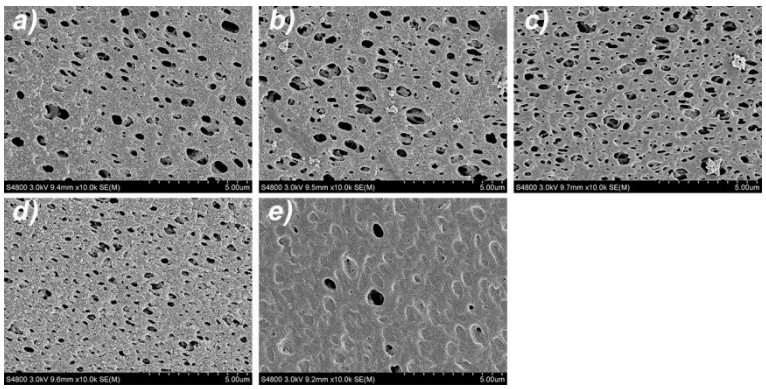

Figure S6 SEM images of different hydrophilic materials coating on poly(ether sulfone) microporous membrane. a) PDA/PEI co-deposition nanoparticles, b) SiO_2 nanoparticles, c) ZnO nanoparticles, d) ZrO_2 nanocoatings, e) $(PDDA/PSS)_5$ LBL nanocoatings.

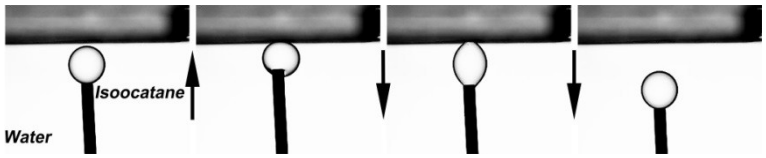

Figure S7 A series of photos taken when an isoocatane droplet was approaching or leaving the PDA/PEI co-deposited poly(ether sulfone) membrane surface in water.

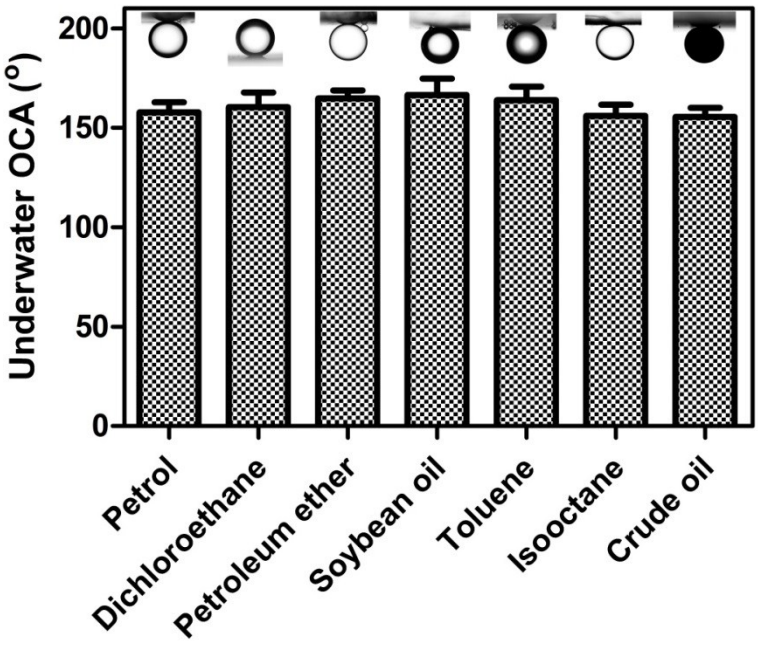

Figure S8 Underwater OCA for different model oils on the CNCs-based nanopapers. The mass thickness of CNCs is 428 mg m^{-2}.

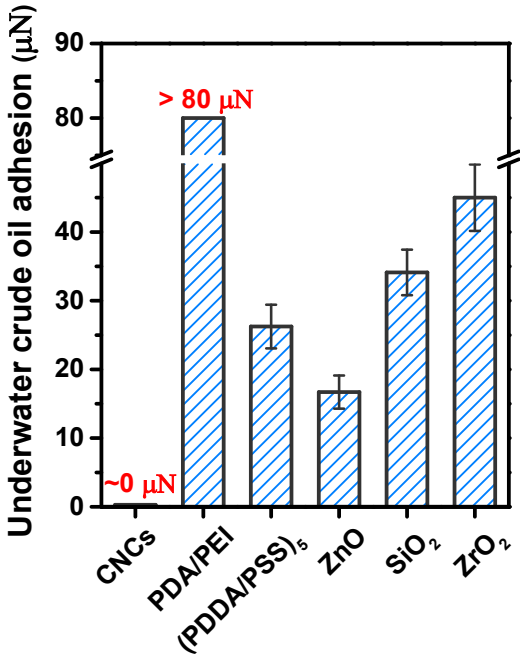

Figure S9 Underwater crude oil adhesive forces of various kinds of superhydrophilic surfaces.

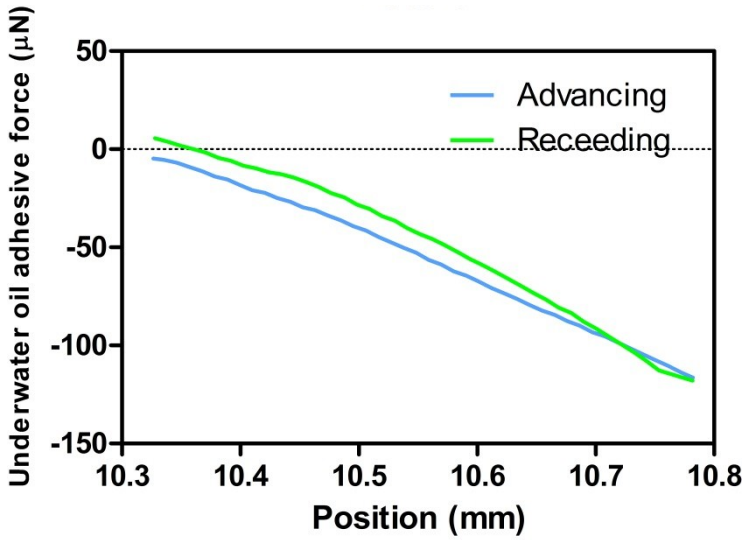

Figure S10 Real-time recorded force-distance curves during the underwater crude oil adhesive force measurements on the CNCs-based nanopapers. The mass thickness of CNCs is 428 mg m^{-2}.

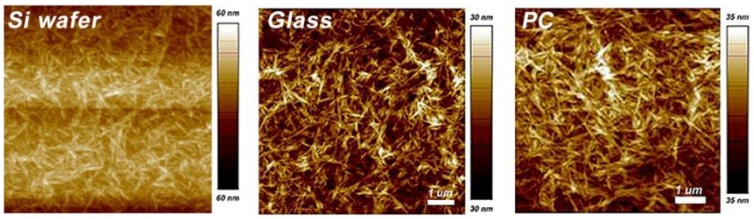

Figure S11 AFM images of different substrates after assemblying CNCs on the silica wafer, glass plate, and polycarbonate (PC) film surfaces. The LBL self-assembly process was repeated 5 times.

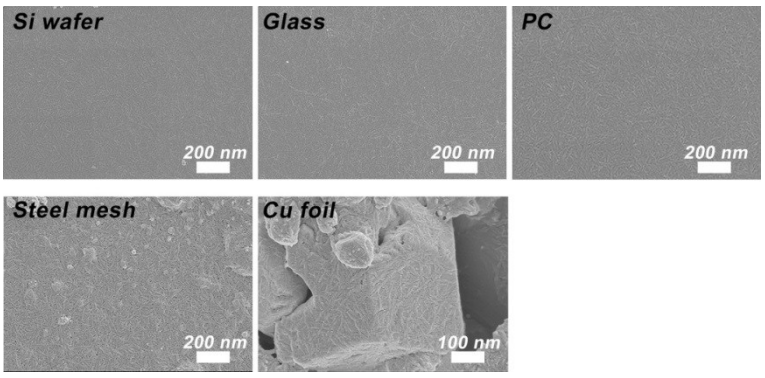

Figure S12 SEM images of different substrates after assemblying CNCs on the surfaces. The LBL self-assembly process was repeated 5 times.

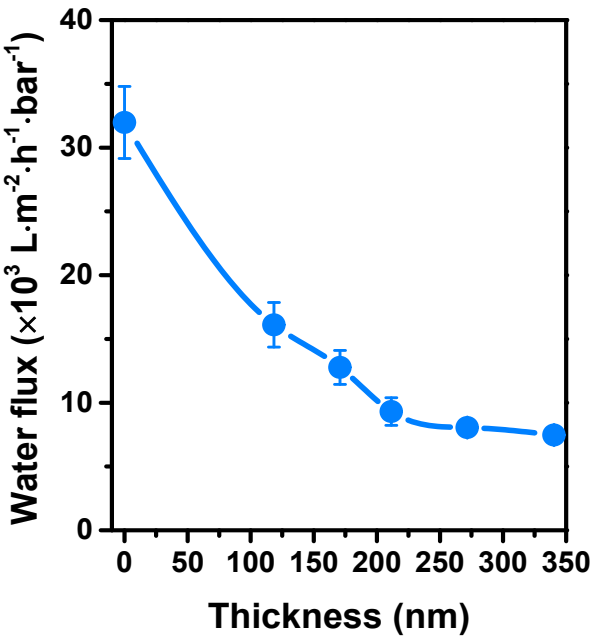

Figure S13 Water permeation flux of the CNCs-based nanopapers with different thicknesses.

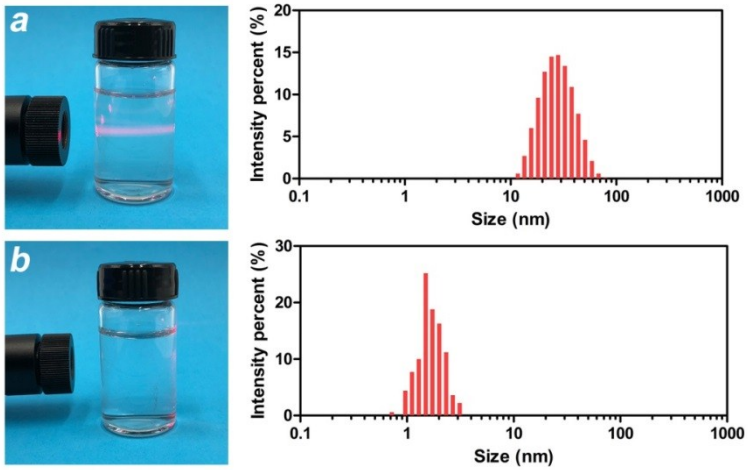

Figure S14 Digital photo and size distribution of the oil droplet of the isooctane-in-water nanoemulsion before (a) and after (b) separation by the CNCs-based nanopapers with a thickness of 165 nm.

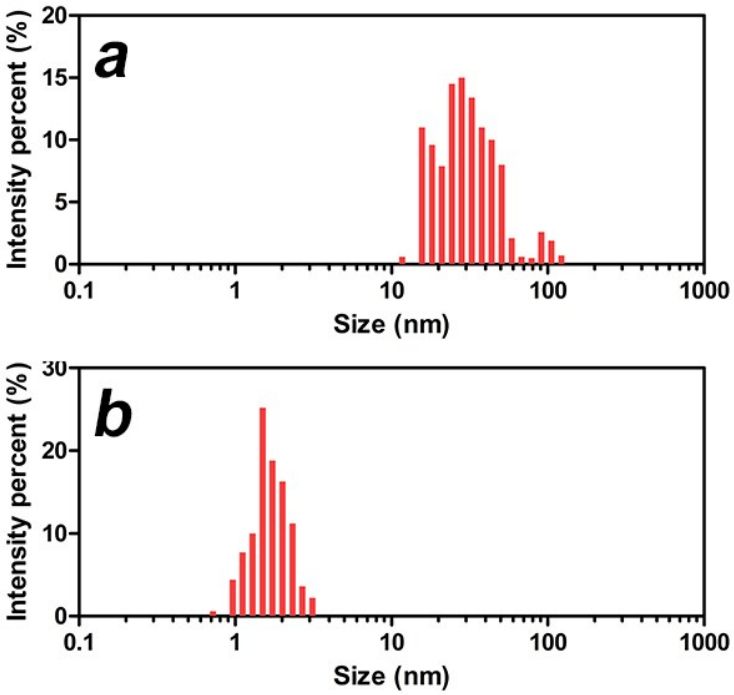

Figure S15 Size distribution of the oil droplet of the dichloroethane-in-water nanoemulsion before (a) and after (b) separation by the CNCs-based nanopapers with a thickness of 165 nm.

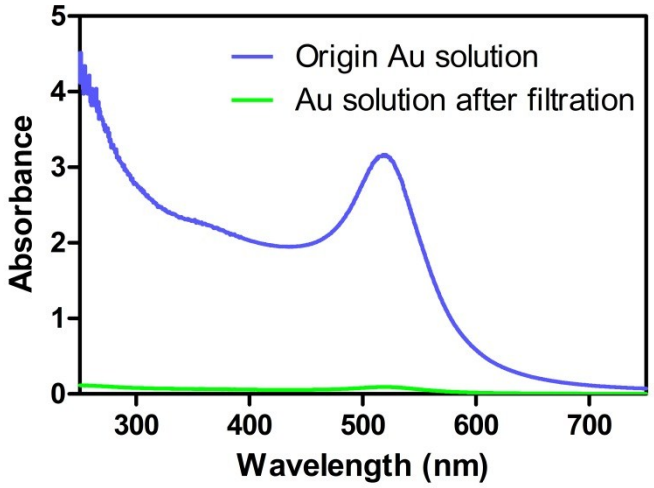

Figure S16 UV-vis spectra of the Au nanoparticle (15 nm) solution before and after filtration by the CNCs-based nanopapers with a thickness of 165 nm.

Figure S17 Schematic diagram of the homemade separation device.